

## Literature Review

**Cite this article:** Fielding AL. (2023) Monte-Carlo techniques for radiotherapy applications II: equipment and source modelling, dose calculations and radiobiology. *Journal of Radiotherapy in Practice*. **22**(e81), 1–6. doi: [10.1017/S1460396923000080](https://doi.org/10.1017/S1460396923000080)

Received: 1 December 2022

Revised: 26 January 2023

Accepted: 3 February 2023

### Key words:

Monte-Carlo simulation; radiotherapy; radiation; dosimetry

### Author for correspondence:

Andrew L. Fielding, School of Chemistry and Physics, Queensland University of Technology (QUT), Brisbane, Australia.  
E-mail: [a.fielding@qut.edu.au](mailto:a.fielding@qut.edu.au)

# Monte-Carlo techniques for radiotherapy applications II: equipment and source modelling, dose calculations and radiobiology

Andrew L. Fielding 

School of Chemistry and Physics, Queensland University of Technology (QUT), Brisbane, Australia

## Abstract

**Introduction:** This is the second of two papers giving an overview of the use of Monte-Carlo techniques for radiotherapy applications.

**Methods:** The first paper gave an introduction and introduced some of the codes that are available to the user wishing to model the different aspects of radiotherapy treatment. It also aims to serve as a useful companion to a curated collection of papers on Monte-Carlo that have been published in this journal.

**Results and Conclusions:** This paper focuses on the application of Monte-Carlo to specific problems in radiotherapy. These include radiotherapy and imaging beam production, brachytherapy, phantom and patient dosimetry, detector modelling and track structure calculations for micro-dosimetry, nano-dosimetry and radiobiology.

## Introduction

This is the second overview paper on the use of Monte-Carlo in radiotherapy. The first part gave an introduction to the Monte-Carlo technique and the different codes that are available for simulating radiotherapy treatments. In this second overview paper on the use of Monte-Carlo for radiotherapy, the main areas of application will be summarised. This includes modelling the production of beams of ionising radiation for radiotherapy and medical imaging, treatment verification, patient dosimetry and radiobiology.

### Radiotherapy and imaging equipment modelling

A common application of the Monte-Carlo method is in the modelling of imaging and radiotherapy equipment such as X-ray tubes, linear accelerators and detectors. For comprehensive reviews of the use of Monte-Carlo techniques for radiotherapy, the reader is referred to the following literature.<sup>1–9</sup> An overview of some of the published work in some of the different areas of radiotherapy now follows.

### X-ray tube modelling

Monte-Carlo techniques have been used to model X-ray tubes in the context of kilo- and ortho-voltage radiotherapy as well as medical and industrial imaging. The modelling of the X-ray tube enables a deeper understanding of the Bremsstrahlung production process in the target as well as the influence of components such as windows, collimators and filters on the spectral and fluence properties of the X-ray beams that are generated.<sup>10,11</sup> Figure 1 shows an example of a simple X-ray tube geometry implemented using the XTUBE component module of the BEAMnrc user code.<sup>12</sup> Information from the manufacturer on the target material (s), thickness (es), angle, electron beam energy and radius and window details can be used to develop the model. Additional collimators, filters and applicators can also be included using other available component modules. X-ray tubes are used for a wide variety of applications, and Monte-Carlo simulation has been applied accordingly. These applications include X-ray tubes in clinical diagnostic CT systems.<sup>13</sup> As part of the Monte-Carlo collection of papers in this journal, Aghdam et al used the MCNP code to model the treatment head of an intraoperative electron radiotherapy accelerator in order to calculate the radiation contamination dose in the area around the device.<sup>14</sup> In another study, the same group investigated the effective SSD dependence on electron energy and applicator size.<sup>15</sup> Al-Ghorabie used the BEAMnrc code to model the XStrahl 150 kV radiotherapy unit. Simulated X-ray spectra, first and second Half-Value Layers (HVLs) and dose profiles were compared to measured data. Measured and simulated spectra were found to agree to ~1% and HVLs differed between 2.3 and 3.6%. Percentage depth doses agreed to within 2% and beam profiles in the range 3–5 % depending on applicator size.<sup>16</sup> At this point, the reader is reminded that Monte-Carlo simulations are highly sensitive to the configuration parameters

© The Author(s), 2023. Published by Cambridge University Press. This is an Open Access article, distributed under the terms of the Creative Commons Attribution licence (<http://creativecommons.org/licenses/by/4.0/>), which permits unrestricted re-use, distribution and reproduction, provided the original article is properly cited.

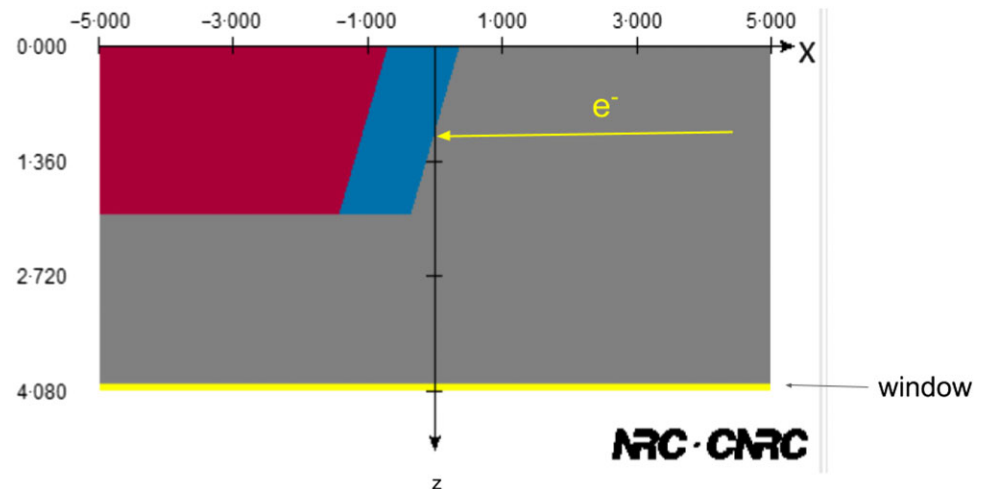


**Figure 1.** Simple X-ray tube model created using the XTUBE component module of the BEAMnrc user code. Grey indicates a vacuum. Blue indicates the tungsten target embedded on the red copper mounting. Axis dimensions are in centimetres.

used for a particular simulation. For this reason, when seeking to reproduce simulations by others, it is important that the exact same settings are used. An important responsibility therefore falls on the authors of research involving Monte-Carlo simulation to include all relevant configuration parameters to enable reproducibility by others.<sup>17</sup>

#### Radiotherapy delivery equipment modelling

Monte-Carlo techniques have been widely used to model clinical electron and X-ray beams, patient dosimetry and imaging systems found in the radiotherapy treatment room. Padilla-Cabal et al compared the MCNPX and BEAMnrc Monte-Carlo models for an Elekta Precise SL-25 photon beam. The MC models were compared to measure dosimetry profile data in homogeneous water and homogeneous phantoms containing air, bone and lung equivalent materials.<sup>18</sup> Toossi et al used the MCNPX code to simulate the 8, 12 and 14 MeV electron beams generated by a Siemens Primus linear accelerator. Simulated dosimetry profile data were compared to measured data for different field sizes including applicators as part of a commissioning process.<sup>19</sup> Monte-Carlo techniques can also be used to model more specialised radiotherapy equipment such as Tomotherapy<sup>20,21</sup> and the Cobalt-60 based Gamma Knife.<sup>22–24</sup> Mahmoudi et al used the BEAMnrc code to model the beam profiles of the individual and 201 combined beams of the Gamma Knife stereotactic radiotherapy system. Simulated data were compared with measured film dosimetry in a plexiglass head phantom for four different collimator sizes, 4, 8, 14 and 18 mm diameter.<sup>25</sup> It is also worth noting that Monte-Carlo techniques have also been used widely for verifying treatment dosimetry through the use of Electronic Portal Imaging Detector (EPID)-based dosimetry.<sup>26–29</sup> The technique can offer an accurate calculation of the portal dose response of the detector for comparison to the measured portal dose.

#### Proton and Heavy Ion beam modelling

Monte-Carlo techniques have been extensively used to model clinical proton and heavy ion beams and their interactions and deposition of dose in patient geometries.<sup>30–33</sup> Zarifi et al used the GATE code to study the depth dose characteristics of mono-energetic proton pencil beams of energies 5–250 MeV in water and obtain the energy–range relationship. Further, the stopping powers of the proton pencil beams in a water phantom were compared to

data from the NIST standard reference database.<sup>34</sup> Zafiri et al performed a study to compare the accuracy of the different physics lists (models) that are available in the GATE code when simulating monoenergetic therapeutic proton pencil beams with energies 5–250 MeV.<sup>35</sup> Chiang et al used TOPAS to model the treatment head of the Mevion HYPERSCAN pencil beam scanning system proton therapy system including the energy modulation system and Adaptive Aperture. Depth doses and in-air spot sizes were found to have good agreement with measured beam data (1 mm and 10 %, respectively). Full-width half maximums and lateral penumbra agreed to within 2 mm.<sup>36</sup>

#### Imaging system modelling

The GATE Monte-Carlo system, introduced in the companion part I review, has been extensively used to model CT and the emission imaging systems (nuclear medicine, PET and SPECT). The reader is directed to an excellent topical review by Sarrut et al that includes comprehensive lists of the commercially available emission tomography imaging systems that have been modelled and compared against experimental data.<sup>37</sup> A number of authors have used Monte-Carlo techniques to model the EPID and cone beam CT imaging systems that are now found on contemporary linear accelerators. This work has included modelling of the X-ray tube and detector systems. A number of authors have modelled a linear accelerator clinical cone beam CT system for the purposes of evaluating patient dosimetry during dosimetry.<sup>38–40</sup> Monte-Carlo has also been used to evaluate and correct for scatter contributions to both megavoltage and kV cone beam CT.<sup>41–45</sup> Monte-Carlo has been widely used for modelling and optimising MV portal imaging systems for both anatomical imaging and dosimetry. Flampouri et al used the EGSnrc codes to optimise a low atomic number (Z) X-ray Bremsstrahlung target and detector for radiotherapy MV imaging.<sup>46</sup> Accurate modelling of the portal imaging detector response has been performed using Monte-Carlo techniques. The calculated portal dose image can then be compared to a measured image as a method of *in-vivo* treatment verification. Parent et al developed a Monte-Carlo model for the Elekta iView GT a-Silicon flat panel imager.<sup>47,48</sup> A different technique based on calculation and measurement of radiological thickness was demonstrated by Kairn et al<sup>26</sup> A number of other authors performed similar studies for Varian liquid ionisation chamber and flat panel imaging detectors<sup>28,49</sup>

## Brachytherapy

While the majority of this overview has focussed on external beam radiotherapy and associated imaging, it is worth noting that Monte-Carlo calculation techniques have been widely used to model the dosimetry of brachytherapy. Many of the Monte-Carlo codes have capabilities for defining the geometries and sources used in brachytherapy, including EGSnrc and its `egs_brachy` user code,<sup>50</sup> MCNP<sup>51,52</sup> and GEANT4.<sup>53–55</sup> For those without GEANT4 experience, brachytherapy simulation capabilities are also offered through the more user-friendly TOPAS and GATE toolkits.<sup>56,57</sup> As part of the Monte-Carlo collection in this journal, Dagli et al compared three different dose calculation algorithms for clinical HDR brachytherapy. The aim was to investigate the accuracy of the BrachyDose Monte-Carlo code in heterogeneous media through a comparison with the Eclipse TG-43 dose calculation tool and the Acuros BV model-based algorithm. Acuros BV and BrachyDose were found to have a good agreement, but significant dose differences were seen with the Eclipse TG-43 dose calculation.<sup>58</sup>

## Dosimetry and treatment verification

The first step in a Monte-Carlo simulation of a radiotherapy treatment involves modelling the production of the beam of ionising radiation as discussed in Sections 2-1, 2-2 and 2-3. The output from the simulation can then be used as an input to the simulation of the interaction of the beam(s) with a patient, phantom or detector. Computed tomography images of patients and phantoms in DICOM format can be used to accurately create a voxelised model of the geometry or specific anatomy, including the different segmented tissues and structures in a patient. Simulation of MV X-ray and electron beams used in radiotherapy requires the use of a CT-electron density calibration curve that provides the relationship between CT number and electron density for the segmented tissues in the voxelised patient model. As part of this process, it is common to simplify the assignment of electron densities so that the complex tissues existing in the human body are categorised into just a few basic types, e.g. soft tissue, lung, bone, and air.

As part of the Monte-Carlo collection of this journal, Zaman et al used the EGSnrc code to model enhanced dynamic wedge deliveries to heterogeneous slab phantoms containing lung and bone heterogeneities in water-equivalent material. The Monte-Carlo results were compared with calculations using the Anisotropic analytical algorithm (AAA) and the Acuros XB algorithms found in the Varian Eclipse treatment planning system.<sup>59</sup> Yabsantia et al. performed a comparison of 6 MV photon small field output factors measured following the TGS-483 code of practice with calculations performed using the EGSnrc Monte-Carlo code. Measured output factors for three different detectors, the IBA-CC01, Sun Nuclear EDGE and IBA-SFD, were corrected using the TG-483 formalism and compared with the Monte-Carlo simulations performed using the `egs_chamber` EGSnrc user code.<sup>60</sup> Vassiliev et al used the BEAMnrc/DOSXYZnrc Monte-Carlo code to study the effect of motion on target dose coverage for lung stereotactic body radiation therapy patients treated with flattening filter-free beams. Fifteen patient plans were re-calculated using 4D-CT data with and without the flattening filter. The target coverage for treatment planning system calculations was compared with the Monte-Carlo for each of the patients.<sup>61</sup> Tanha et al investigated the accuracy of a collapsed cone convolution and ETAR algorithm through comparison with a BEAMnrc Monte-Carlo model of the Varian 2100 C/D 18V photon beam. Dosimetric

comparisons were made for a pituitary gland treatment planned on a rando-phantom. Differences between the Monte-Carlo and collapsed cone and ETAR were found to be up to 6 and 10 %, respectively.<sup>62</sup> Nithiyantham et al compared the XVMC Monte-Carlo dose calculation algorithm found in the commercial Monaco treatment planning system to measured doses for small field sizes (8 × 8 up to 40 × 40 mm) in soft tissue equivalent phantoms containing lung and bone heterogeneities. They observed deviations for the smallest field sizes in and around the soft-tissue heterogeneity interfaces.<sup>63</sup> Mamballikalam et al investigated the dosimetry of 6 MV flattening filter-free small fields measured with three different dosimeters, the IBA CC01 pinpoint chamber, the IBA stereotactic field diode and the PTW microDiamond. Measured doses were compared with calculated doses obtained using the PRIMO Monte-Carlo code. The work showed that for field sizes below 1 × 1 cm perturbation and volume averaging corrections should be applied.<sup>64</sup> Chow and Owrangi used the BEAMnrc code to investigate the mucosal dose in the oral and nasal cavity and its dependence on beam energy, beam angle, mucosal thickness and the backscatter from neighbouring bone for small 6 and 18 MV fields generated by a Varian 21 EX accelerator.<sup>65</sup> Acar et al compared the accuracy of the Varian Eclipse electron Monte-Carlo dose calculation algorithm with the Gaussian pencil beam algorithm. The work focussed on the ability of both algorithms to calculate peripheral doses for 6 electron beam energies ranging from 6 to 22 MeV. Calculated peripheral doses were compared with measured (ion chamber and EBT film) for three field sizes, 6 × 6, 10 × 10 and 25 × 25 cm. Differences of up to 8.8 % between Gaussian pencil beam and measurements were reduced to less than 4.3 % for electron Monte-Carlo and measurement.<sup>66</sup> Abdul Aziz et al used a BEAMnrc model of a 6 MV photon beam generated by a Siemens Primus linear accelerator to investigate the effect of artefacts due to a titanium hip prosthesis in CT data on the dose distribution in and around the prosthesis.<sup>67</sup>

## Micro/Nano-dosimetry, radio-chemistry and radiobiology

The macroscopic modelling of radiation production and dose deposition Monte-Carlo can also be used to model radiation interactions on the micro and nano-length scale. For these applications, a track structure paradigm, rather than the condensed history technique, is used that models the individual low energy charged particle interactions at the much shorter length scales. GEANT4 has led the way with this through the development of the GEANT4-DNA toolkit,<sup>68,69</sup> an extension to the GEANT4 toolkit. GEANT4-DNA has been validated for the modelling of the low energy physics interactions in water as well as the production and subsequent interactions of the reactive chemical species following the radiolysis of water.<sup>70,71</sup> From a radiobiological perspective, the DNA damage produced by ionising radiation has also been modelled<sup>72</sup> using GEANT4-DNA. Validation of these microscopic track structure simulation codes for different ionising radiations has been performed against laboratory experiments and in comparison with other independent Monte-Carlo codes.<sup>73</sup> As has already been indicated, for those without C++ expertise, all these GEANT4-DNA capabilities for low energy physics, chemistry and radiobiology are accessible through the user-friendly TOPAS-nBio toolkit.<sup>74–77</sup> Figure 2(a) shows a TOPAS simulation of the simulated tracks of 50 keV electrons traversing a spherical cell model containing mitochondria and gold nanoparticles. Similar models have been used to investigate the nano-scale and radiobiological interactions underpinning dose enhancement with nano-particles

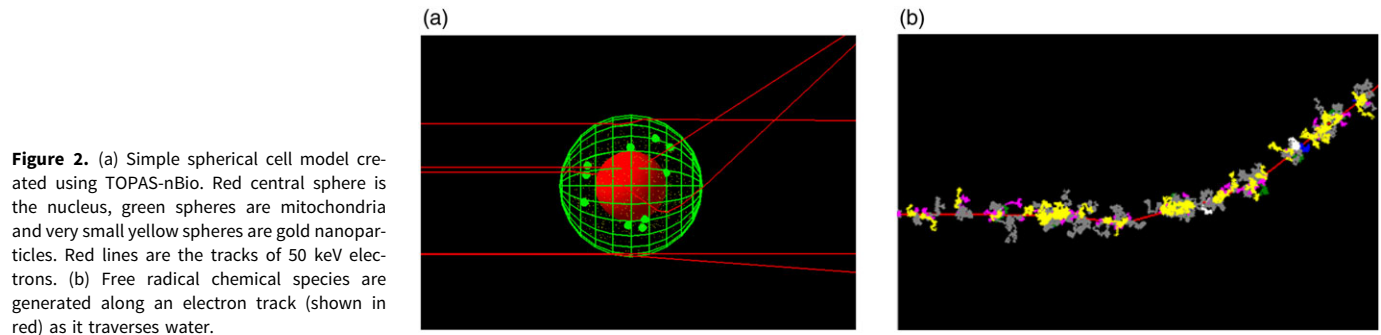


**Figure 2.** (a) Simple spherical cell model created using TOPAS-nBio. Red central sphere is the nucleus, green spheres are mitochondria and very small yellow spheres are gold nanoparticles. Red lines are the tracks of 50 keV electrons. (b) Free radical chemical species are generated along an electron track (shown in red) as it traverses water.

and more recently high dose-rate FLASH radiotherapy delivery,<sup>78,79</sup> both using TOPAS-nBio. In the Monte-Carlo collection of this journal, Belamri et al used GEANT4 to investigate the potential dose enhancement effect of gold, silver or platinum nano-particles when irradiated with proton beams with energies typical of those used for brain treatments.<sup>80</sup>

The TOPAS-nBio code also has the capability to model the chemistry following the physical processes. This includes the free radical chemical species production (e.g. H<sup>+</sup> and OH<sup>-</sup> ions) plus the subsequent diffusion of these species through the cell geometry.<sup>75</sup> Figure 2(b) shows an example of the chemical species generated along an electron track as it traverses water. The motion of the chemical species can then be modelled as a function of time.

These radiobiological level simulations of the physics and chemistry of ionising radiation interactions are an extremely powerful tool that can play a crucial role in increasing our understanding of the radiobiology of ionising radiation at the cellular length scale.

## Conclusions

Monte-Carlo is a powerful tool for simulating the transport of ionising radiation as it traverses matter. This feature has resulted in the statistical technique being widely and successfully applied to the modelling and simulation of radiotherapy treatments, with most modern radiotherapy treatment planning systems offering a Monte-Carlo algorithm for at least electron beams. A number of different codes are available for free download and require little prior programming experience. These codes enable the user to model the complex geometries in radiotherapy and imaging equipment and the beams they produce. These simulated beams can then be used to accurately model the dosimetry in phantoms, patients, detectors and the radiobiology at smaller micro- and nano-length scales. The Monte-Carlo method has a rich history in the development of new radiation production equipment and detector technology as well as improving our understanding of ionising radiation interactions in human tissues. The continued research into the development of Monte-Carlo codes and algorithms for radiotherapy applications would seem to indicate it will have an increasing role to play well into the foreseeable future.

## References

- Verhaegen F, Seuntjens J. Monte Carlo modelling of external radiotherapy photon beams. *Phys Med Biol* 2003; 48 (21): R107–R164.
- Park H, Paganetti H, Schuemann J, Jia X, Min CH. Monte Carlo methods for device simulations in radiation therapy. *Phys Med Biol* 2021; 66 (18): 18TR01. doi: [10.1088/1361-6560/ac1dlf](https://doi.org/10.1088/1361-6560/ac1dlf)
- Andreo P. Monte Carlo simulations in radiotherapy dosimetry. *Radiat Oncol* 2018; 13 (1): 121.
- Chetty IJ, Curran B, Cygler JE, et al. Report of the AAPM Task Group No. 105: issues associated with clinical implementation of Monte Carlo-based photon and electron external beam treatment planning. *Med Phys* 2007; 34 (12): 4818–4853.
- Brualla L, Rodriguez M, Lallena AM. Monte Carlo systems used for treatment planning and dose verification. *Strahlenther Onkol* 2016; 193 (4): 243. doi: [10.1007/s00066-016-1075-8](https://doi.org/10.1007/s00066-016-1075-8)
- Reynaert N, van der Marck SC, Schaart DR, et al. Monte Carlo treatment planning for photon and electron beams. *Radiat Phys Chem* 2007; 76 (4): 643–686.
- Rogers DW. Fifty years of Monte Carlo simulations for medical physics. *Phys Med Biol* 2006; 51 (13): R287–R301.
- Seco J, Verhaegen F. *Monte Carlo Techniques in Radiation Therapy: Applications to Dosimetry, Imaging, and Preclinical Radiotherapy*. Boca Raton: Taylor & Francis Group, 2021.
- Verhaegen F, Seco J. *Monte Carlo Techniques in Radiation Therapy: Introduction, Source Modelling, and Patient Dose Calculations*. Boca Raton: Taylor & Francis Group, 2021.
- Poludniowski GG, Evans PM. Calculation of x-ray spectra emerging from an x-ray tube. Part I. electron penetration characteristics in x-ray targets. *Med Phys* 2007; 34 (6): 2164–2174.
- Poludniowski GG. Calculation of x-ray spectra emerging from an x-ray tube. Part II. X-ray production and filtration in x-ray targets. *Med Phys* 2007; 34 (6): 2175–2186.
- Rogers DW, Faddegon BA, Ding GX, Ma CM, We J, Mackie TR. BEAM: a Monte Carlo code to simulate radiotherapy treatment units. *Med Phys* 1995; 22 (5): 503–524.
- Bazalova M, Verhaegen F. Monte Carlo simulation of a computed tomography x-ray tube. *Phys Med Biol* 2007; 52 (19): 5945–5955.
- Aghdam SRH, Siavashpour Z, Aghamiri SMR, Mahdavi SR, Nafisi N. Evaluating the radiation contamination dose around a high dose per pulse intraoperative radiotherapy accelerator: a Monte Carlo study. *J Radiother Pract* 2020; 19 (3): 265–276.
- Aghdam MRH, Baghani HR, Mahdavi SR, Aghamiri SMR, Akbari ME. Monte Carlo study on effective source to surface distance for electron beams from a mobile dedicated IORT accelerator. *J Radiother Pract* 2017; 16 (1): 29–37.
- Al-Ghorabie FHH. Experimental measurements and Monte Carlo modelling of the XSTRAHL 150 superficial X-ray therapy unit. *J Radiother Practice* 2015; 14 (1): 43–55.
- Sechopoulos I, Rogers DWO, Bazalova-Carter M, et al. RECORDS: improved reporting of Monte Carlo radiation transport studies: report of the AAPM Research Committee Task Group 268. *Med Phys* 2018; 45 (1): e1–e5.
- Padilla-Cabal F, Pérez-Liva M, Lara E, Alfonso R, Lopez-Pino N. Monte Carlo calculations of an Elekta Precise SL-25 photon beam model. *J Radiother Pract* 2015; 14 (3): 1–12.



19. Bahreyni Toossi MT, Ghorbani M, Akbari F, Sabet LS, Mehrpouyan M. Monte Carlo simulation of electron modes of a Siemens Primus linac (8, 12 and 14 MeV). *J Radiother Pract* 2013; 12 (4): 352–359.
20. Zhao YL, Mackenzie M, Kirkby C, Fallone BG. Monte Carlo evaluation of a treatment planning system for helical tomotherapy in an anthropomorphic heterogeneous phantom and for clinical treatment plans. *Med Phys* 2008; 35 (12): 5366–5374.
21. Zhao YL, Mackenzie M, Kirkby C, Fallone BG. Monte Carlo calculation of helical tomotherapy dose delivery. *Med Phys* 2008; 35 (8): 3491.
22. Moskvina V, DesRosiers C, Papiez L, Timmerman R, Randall M, DesRosiers P. Monte Carlo simulation of the Leksell Gamma Knife: I. Source modelling and calculations in homogeneous media. *Phys Med Biol* 2002; 47 (12): 1995–2011.
23. Moskvina V, Timmerman R, DesRosiers C, et al. Monte Carlo simulation of the Leksell Gamma Knife: II. Effects of heterogeneous versus homogeneous media for stereotactic radiosurgery. *Phys Med Biol* 2004; 49 (21): 4879–4895.
24. Junios J, Irhas I, Novitrian N, et al. Characterization of Gamma Knife Perfexion™ source based on Monte Carlo simulation. *Radiol Phys Technol* 2020; 13 (4): 398–404.
25. Mahmoudi A, Shirazi A, Geraily G, Nia TH, Bakhshi M, Maleki M. Penumbra width determination of single beam and 201 beams of Gamma Knife machine model 4C using Monte Carlo simulation. *J Radiother Pract* 2019; 18 (1): 82–87.
26. Kairn T, Cassidy D, Sandford PM, Fielding AL. Radiotherapy treatment verification using radiological thickness measured with an amorphous silicon electronic portal imaging device: monte Carlo simulation and experiment. *Phys Med Biol* 2008; 53 (14): 3903–3919.
27. Chin PW, Spezi E, Lewis DG. Monte Carlo simulation of portal dosimetry on a rectilinear voxel geometry: a variable gantry angle solution. *Phys Med Biol* 2003; 48 (16): N231–N238.
28. Siebers JV, Kim JO, Ko L, Keall PJ, Mohan R. Monte Carlo computation of dosimetric amorphous silicon electronic portal images. *Med Phys* 2004; 31 (7): 2135–2146.
29. Herwiningsih S, Hanlon P, Fielding A. Sensitivity of an Elekta iView GT a-Si EPID model to delivery errors for pre-treatment verification of IMRT fields. *Australas Phys Eng Sci Med* 2014; 37 (4): 763–770.
30. Rahman M, Bruza P, Lin Y, Gladstone DJ, Pogue BW, Zhang R. Producing a beam model of the Varian ProBeam Proton Therapy System using TOPAS Monte Carlo Toolkit. *Med Phys* 2020; 47 (12): 6500–6508.
31. Tourovsky A, Lomax AJ, Schneider U, Pedroni E. Monte Carlo dose calculations for spot scanned proton therapy. *Phys Med Biol* 2005; 50 (5): 971–981.
32. Paganetti H, Jiang H, Parodi K, Slopssema R, Engelsman M. Clinical implementation of full Monte Carlo dose calculation in proton beam therapy. *Phys Med Biol* 2008; 53 (17): 4825–4853.
33. Vedelago J, Geser FA, Muñoz ID, Stabilini A, Yukihara EG, Jäkel O. Assessment of secondary neutrons in particle therapy by Monte Carlo simulations. *Phys Med Biol* 2022; 67 (1): 015008. doi: [10.1088/1361-6560/ac431b](https://doi.org/10.1088/1361-6560/ac431b)
34. Zarifi S, Ahangari HT, Jia SB, Tajik-Mansoury MA, Najafzadeh M, Firouzjaei MP. Bragg peak characteristics of proton beams within therapeutic energy range and the comparison of stopping power using the GATE Monte Carlo simulation and the NIST data. *J Radiother Pract* 2020; 19 (2): 173–181.
35. Zarifi S, Ahangari HT, Jia SB, Tajik-Mansoury MA. Validation of GATE Monte Carlo code for simulation of proton therapy using National Institute of Standards and Technology library data. *J Radiother Pract* 2019; 18 (1): 38–45.
36. Chiang BH, Bunker A, Jin H, Ahmad S, Chen Y. Developing a Monte Carlo model for MEVION S250i with HYPERSCAN and Adaptive Aperture™ pencil beam scanning proton therapy system. *J Radiother Pract* 2021; 20 (3): 279–286.
37. Sarrut D, Bala M, Bardiès M, et al. Advanced Monte Carlo simulations of emission tomography imaging systems with GATE. *Phys Med Biol* 2021; 66 (10): 10TR03. doi: [10.1088/1361-6560/abf276](https://doi.org/10.1088/1361-6560/abf276)
38. Downes P, Jarvis R, Radu E, Kawrakow I, Spezi E. Monte Carlo simulation and patient dosimetry for a kilovoltage cone-beam CT unit. *Med Phys* 2009; 36 (9): 4156–4167.
39. Ding GX, Duggan DM, Coffey CW. Accurate patient dosimetry of kilovoltage cone-beam CT in radiation therapy. *Med Phys* 2008; 35 (3): 1135–1144.
40. Spezi E, Downes P, Radu E, Jarvis R. Monte Carlo simulation of an x-ray volume imaging cone beam CT unit. *Med Phys* 2009; 36 (1): 127–136.
41. Spies L, Ebert M, Groh BA, Hesse BM, Bortfeld T. Correction of scatter in megavoltage cone-beam CT. *Phys Med Biol* 2001; 46 (3): 821–833.
42. Bootsma GJ, Verhaegen F, Jaffray DA. The effects of compensator and imaging geometry on the distribution of x-ray scatter in CBCT. *Med Phys* 2011; 38 (2): 897–914.
43. Poludniowski G, Evans PM, Hansen VN, Webb S. An efficient Monte Carlo-based algorithm for scatter correction in keV cone-beam CT. *Phys Med Biol* 2009; 54 (12): 3847–3864.
44. Mosleh-Shirazi MA, Swindell W, Evans PM. Optimization of the scintillation detector in a combined 3D megavoltage CT scanner and portal imager. *Med Phys* 1998; 25 (10): 1880–1890.
45. Swindell W, Evans PM. Scattered radiation in portal images: a Monte Carlo simulation and a simple physical model. *Med Phys* 1996; 23 (1): 63–73.
46. Flampouri S, Evans PM, Verhaegen F, Nahum AE, Spezi E, Partridge M. Optimization of accelerator target and detector for portal imaging using Monte Carlo simulation and experiment. *Phys Med Biol* 2002; 47 (18): 3331–3349.
47. Parent L, Fielding AL, Dance DR, Seco J, Evans PM. Amorphous silicon EPID calibration for dosimetric applications: comparison of a method based on Monte Carlo prediction of response with existing techniques. *Phys Med Biol* 2007; 52 (12): 3351–3368.
48. Parent L, Seco J, Evans PM, Fielding A, Dance DR. Monte Carlo modelling of a-Si EPID response: the effect of spectral variations with field size and position. *Med Phys* 2006; 33 (12): 4527–4540.
49. Spezi E, Lewis DG. Full forward Monte Carlo calculation of portal dose from MLC collimated treatment beams. *Phys Med Biol* 2002; 47 (3): 377–390.
50. Chamberland MJP, Taylor REP, Rogers DWO, Thomson RM. Egs\_brachy: a versatile and fast Monte Carlo code for brachytherapy. *Phys Med Biol* 2016; 61 (23): 8214–8231.
51. Solberg TD, DeMarco JJ, Chetty IJ, et al. A review of radiation dosimetry applications using the MCNP Monte Carlo code. *Radiochim Acta* 2001; 89 (4–5): 337–355.
52. Zaker N, Zehtabian M, Sina S, Koontz C, Meigooni AS. Comparison of TG-43 dosimetric parameters of brachytherapy sources obtained by three different versions of MCNP codes. *J Appl Clin Med Phys* 2016; 17 (2): 379–390.
53. Enger SA, Landry G, D'Amours M, et al. Layered mass geometry: a novel technique to overlay seeds and applicators onto patient geometry in Geant4 brachytherapy simulations. *Phys Med Biol* 2012; 57 (19): 6269–6277.
54. Poon E, DeBlois F, Devic S, Vuong T, Verhaegen F. Monte Carlo modeling of a novel brachytherapy applicator for rectal cancer treatment using GEANT4. *Radiother Oncol* 2005; 76: S27–S28.
55. Landry G, Reniers B, Pignol JP, Beaulieu L, Verhaegen F. The difference of scoring dose to water or tissues in Monte Carlo dose calculations for low energy brachytherapy photon sources. *Med Phys* 2011; 38 (3): 1526–1533.
56. Sarrut D, Bardiès M, Bousson N, et al. A review of the use and potential of the GATE Monte Carlo simulation code for radiation therapy and dosimetry applications. *Med Phys* 2014; 41 (6): 064301.
57. Berumen F, Ma Y, Ramos-Méndez J, Perl J, Beaulieu L. Validation of the TOPAS Monte Carlo toolkit for HDR brachytherapy simulations. *Brachytherapy* 2021; 20 (4): 911–921.
58. Dagli A, Yurt F, Yegin G. Evaluation of BrachyDose Monte Carlo code for HDR brachytherapy: dose comparison against Acuros®BV and TG-43 algorithms. *J Radiother Pract* 2020; 19 (1): 76–83.
59. Zaman A, Kakakel MB, Hussain A. A comparison of Monte Carlo, anisotropic analytical algorithm (AAA) and Acuros XB algorithms in assessing

- dosimetric perturbations during enhanced dynamic wedged radiotherapy deliveries in heterogeneous media. *J Radiother Pract* 2019; 18 (1): 75–81.
60. Yabsantia S, Suriyapee S, Phaisangittisakul N, Oonsiri S, Sanghangthum T, Seuntjens J. Investigation of field output factors using IAEA-AAPM TRS-483 code of practice recommendations and Monte Carlo simulation for 6 MV photon beams. *J Radiother Pract* 2023; 22: 1–6.
  61. Vassiliev ON, Peterson CB, Chang JY, Mohan R. Monte Carlo evaluation of target dose coverage in lung stereotactic body radiation therapy with flattening filter-free beams. *J Radiother Pract* 2022; 21 (1): 81–87.
  62. Tanha K, Mahdavi SR, Geraily G. Comparison of CCC and ETAR dose calculation algorithms in pituitary adenoma radiation treatment planning: Monte Carlo evaluation. *J Radiother Pract* 2014; 13 (4): 447–455.
  63. Nithiyantham K, Mani GK, Raju S, et al. Characterisation of small photon field outputs in a heterogeneous medium using X-ray voxel Monte Carlo dose calculation algorithm. *J Radiother Pract* 2018; 17 (1): 114–123.
  64. Mamballikalam G, Senthilkumar S, Jayadevan PM, et al. Evaluation of dosimetric parameters of small fields of 6 MV flattening filter free photon beam measured using various detectors against Monte Carlo simulation. *J Radiother Pract* 2021; 20 (3): 332–339.
  65. Chow JCL, Owringi AM. Monte Carlo study on mucosal dose in oral and nasal cavity using photon beams with small field. *J Radiother Pract* 2011; 10 (4): 261–271.
  66. Acar H, Caglar M, Altinok AY. Experimental validation of peripheral dose distribution of electron beams for eclipse electron Monte Carlo algorithm. *J Radiother Pract* 2018; 17 (3): 279–288.
  67. Abdul Aziz MZ, Mohd Kamarulzaman FN, Mohd Termizi NA, Abdul Raof N, Tajuddin AA. Effects of density from various hip prosthesis materials on 6 MV photon beam: a Monte Carlo study. *J Radiother Pract* 2017; 16 (2): 155–160.
  68. Incerti S, Baldacchino G, Bernal M, et al. The Geant4-DNA project. *Int J Model Simulat Sci Computing* 2010; 1 (2): 157–178.
  69. Incerti S, Douglass M, Penfold S, Guatelli S, Bezak E. Review of Geant4-DNA applications for micro and nanoscale simulations. *Phys Med* 2016; 32 (10): 1187–1200.
  70. Bernal MA, Bordage MC, Brown JMC, et al. Track structure modeling in liquid water: a review of the Geant4-DNA very low energy extension of the Geant4 Monte Carlo simulation toolkit. *Phys Med* 2015; 31 (8): 861–874.
  71. Peukert D, Incerti S, Kempson I, et al. Validation and investigation of reactive species yields of Geant4-DNA chemistry models. *Med Phys* 2019; 46 (2): 983–998.
  72. Sakata D, Belov O, Bordage MC, et al. Fully integrated Monte Carlo simulation for evaluating radiation induced DNA damage and subsequent repair using Geant4-DNA. *Sci Rep* 2020; 10 (1): 20788.
  73. Kyriakou I, Sakata D, Tran HN, et al. Review of the Geant4-DNA Simulation Toolkit for Radiobiological Applications at the Cellular and DNA Level. *Cancers* 2021; 14 (1): 35. doi: [10.3390/cancers14010035](https://doi.org/10.3390/cancers14010035)
  74. Schuemann J, McNamara AL, Ramos-Méndez J, et al. TOPAS-nBio: an Extension to the TOPAS Simulation Toolkit for Cellular and Sub-cellular Radiobiology. *Radiat Res* 2019; 191 (2): 125–138.
  75. Ramos-Méndez J, Perl J, Schuemann J, McNamara A, Paganetti H, Faddegon B. Monte Carlo simulation of chemistry following radiolysis with TOPAS-nBio. *Phys Med Biol* 2018; 63 (10): 105014.
  76. McNamara A, Geng C, Turner R, et al. Validation of the radiobiology toolkit TOPAS-nBio in simple DNA geometries. *Phys Med* 2017; 33: 207–215.
  77. Zhu H, McNamara AL, Ramos-Mendez J, et al. A parameter sensitivity study for simulating DNA damage after proton irradiation using TOPAS-nBio. *Phys Med Biol* 2020; 65 (8): 085015.
  78. Rudek B, McNamara A, Ramos-Méndez J, Byrne H, Kuncic Z, Schuemann J. Radio-enhancement by gold nanoparticles and their impact on water radiolysis for x-ray, proton and carbon-ion beams. *Phys Med Biol* 2019; 64 (17): 175005.
  79. Ramos-Méndez J, Domínguez-Kondo N, Schuemann J, McNamara A, Moreno-Barbosa E, Faddegon B. LET-dependent intertrack yields in proton irradiation at ultra-high dose rates relevant for FLASH therapy. *Radiat Res* 2020; 194 (4): 351–362.
  80. Belamri C, Dib ASA, Belbachir AH. Monte Carlo simulation of proton therapy using bio-nanomaterials. *J Radiother Pract*; Cambridge 2016; 15 (3): 290–295.